nature catalysis

Perspective

https://doi.org/10.1038/s41929-023-01082-4

Different distributions of multi-carbon products in CO_2 and CO electroreduction under practical reaction conditions

Received: 15 November 2022

Accepted: 8 November 2023

Published online: 20 December 2023

Check for updates

Jung Yoon 'Timothy' Kim [1,4], Chase Sellers[1,4], Shaoyun Hao[1], Thomas P. Senftle [1] ✉ & Haotian Wang [1,2,3] ✉

Product selectivity differences between the electroreduction of CO_2 and CO under practical current densities are a widely encountered phenomenon that is rarely emphasized or investigated in the field. In this Perspective we have systematically gathered and structured data pertaining to CO_2 and CO electroreduction to underscore the disparities in multi-carbon product formation. In addition, we propose that contributions of the microenvironment and a change in the local pH caused by the formation of carbonate/bicarbonate ions are among the most viable reasons behind such differences in electrochemical performance. Investigating the in situ microenvironment during the electrolysis of CO_2 compared with CO will deepen the mechanistic understanding of different reaction pathways and reveal fundamental insights that may facilitate catalyst design and device-engineering strategies.

The high demand for technologies that use renewable energy to mitigate climate change has made the electrochemical CO_2 reduction reaction (CO_2RR) a focal point of international research efforts in carbon utilization and the renewable manufacture of chemicals[1]. The CO_2RR is a promising technology that provides sustainable methods of utilizing, storing and transporting renewable electricity in the form of liquid fuels and other chemical feedstocks such as formic acid, acetic acid, ethanol, propanol and ethylene[2–5]. Over the past few decades, substantial progress in the CO_2RR field has been realized via the integration of catalyst design and device engineering. Although a plethora of recently reported catalytic materials have enabled the increasingly selective injection of electrons into CO_2 rather than competing H_2O molecules, the production of multi-carbon products at considerable current densities and Faradaic efficiency (FE) values remains exclusive to copper-based catalysts. Many experimental and mechanistic investigations have focused on tuning the Cu catalysts or elucidating the mechanistic details of the multi-carbon (C_{2+}) production network for enhancing the selectivity towards C_{2+} over C_1 products[6–8]. In the production of C_{2+} products, researchers have widely accepted that surface-bound CO (CO*) serves as a key reaction intermediate for the subsequent C–C coupling towards multi-carbon products[9]. As such, increasing the coverage of CO* has a direct impact on improving the selectivity towards C_{2+} products[10,11].

Since CO* serves as a key reaction intermediate in the CO_2RR to multi-carbon products, to optimize the overall energy efficiency, researchers have proposed decoupling the one-step CO_2-to-C_{2+} reaction into two independent steps: CO_2 to CO and CO to C_{2+} products (Fig. 1a)[12–14]. This cascade reaction design presents attractive advantages when compared with the direct one-step conversion of CO_2. First, the electrochemical CO reduction reaction (CORR) undergoes the C–C coupling reaction more readily compared with the CO_2RR, yielding high C_{2+} product selectivity under relatively low reduction overpotentials[15,16]. For example, the CORR can avoid the generation of formic acid, a common C_1 side product, during direct CO_2RR-to-C_{2+} electrolysis. Second, the CORR can operate under highly alkaline conditions and without any concerns of CO_2 absorption or crossover issues, as is the case for the CO_2RR (ref. 17). These conditions promote C_{2+} selectivity and suppress the hydrogen evolution reaction (HER). A recent CORR

[1]Department of Chemical and Biomolecular Engineering, Rice University, Houston, TX, USA. [2]Department of Materials Science and NanoEngineering, Rice University, Houston, TX, USA. [3]Department of Chemistry, Rice University, Houston, TX, USA. [4]These authors contributed equally: Jung Yoon 'Timothy' Kim, Chase Sellers. ✉e-mail: tsenftle@rice.edu; htwang@rice.edu

https://doi.org/10.1038/s41929-023-01082-4

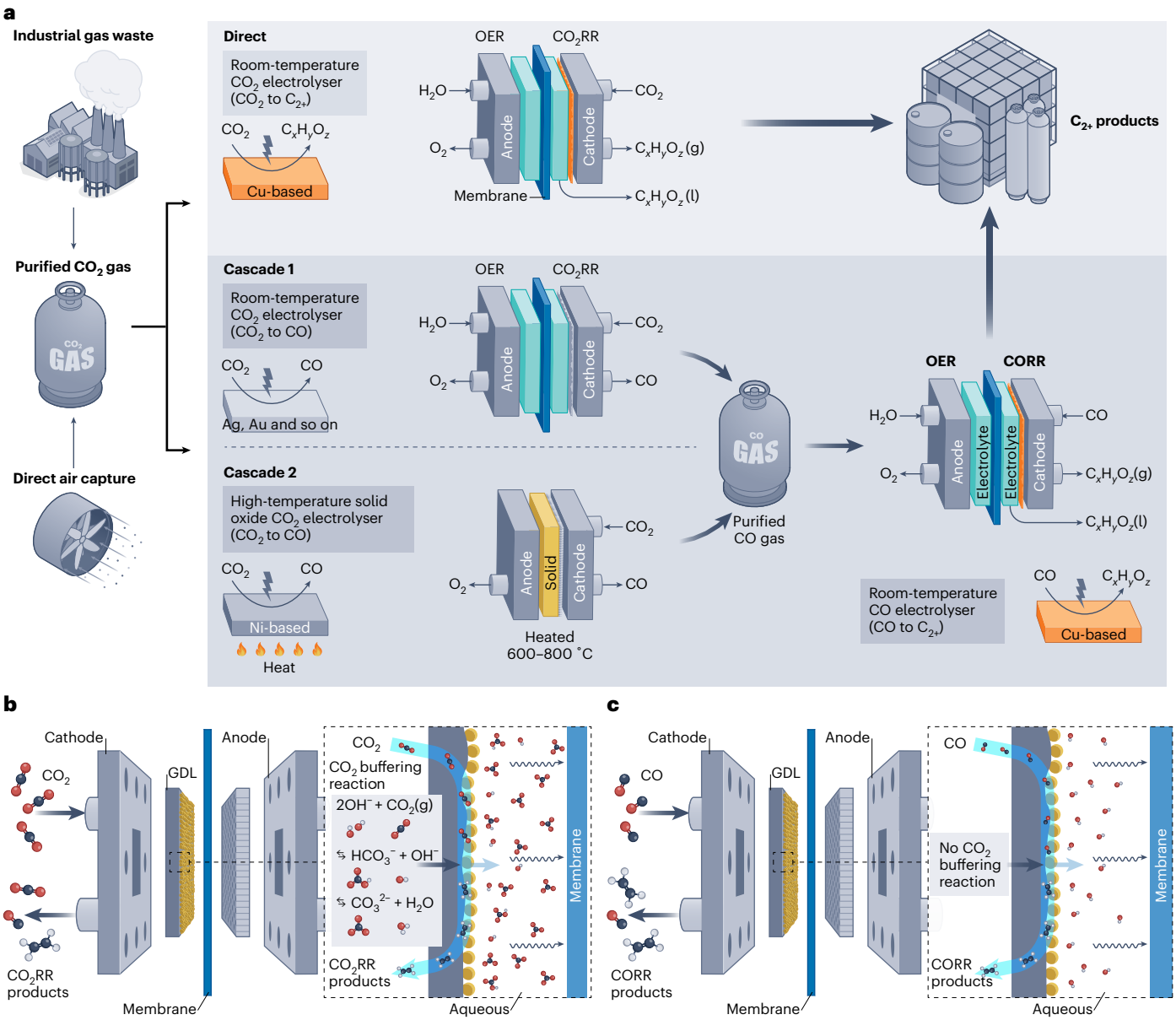

Fig. 1 | Schematics of different reaction design pathways and MEA devices for the $CO_{(2)}$RR. a, CO_2RR electrolyser setups for multi-carbon products can be divided broadly into one-step direct electroreduction and two-step cascade electrolyser designs. OER, oxygen evolution reaction. **b**, CO_2RR in MEA device showing the chemical reaction between generated OH^- and CO_2 to form bicarbonate/carbonate ions (HCO_3^-/CO_3^{2-}). The surface of the catalyst is heavily populated by carbonate ions, which are then transported towards the anode. Atom code: C, black; O, red; H, white. GDL, gas diffusion layer. **c**, CORR in MEA device showing no pH buffering reactions and the catalyst surface being heavily populated with generated OH^- ions.

study achieved over 90% selectivity at an industrially relevant current density of up to 1 A cm^{-2} (ref. 15). Third, using CO-selective catalysts such as Ag, Au and the Ni single-atom catalyst, the CO_2RR to CO step can yield commercially relevant selectivity, activity and stability in membrane electrode assembly (MEA) devices at room temperature (Fig. 1a). In addition, high-temperature solid oxide electrolysis cells (SOECs) have already been used industrially to successfully reduce CO_2 to CO in large quantities[18,19]. The SOEC operates at a high temperature of around 800 °C and uses Ni-based catalysts to achieve thousands of hours of stable CO production from CO_2 without any liquid electrolyte input (Fig. 1a). More importantly, the SOEC device enables operation without the formation of carbonate ions, which facilitates the high utilization of carbon by limiting carbonate formation as observed in room-temperature CO_2 electrolysers. The cascade-reactor design demonstrated by Ozden et al. has shown the energy advantage of coupling an SOEC with a CORR electrolyser. In that work, the authors estimated an energy intensity of 138 GJ per ton of ethylene produced for the cascade system while they estimated energy intensity of 267 GJ per ton of ethylene produced via direct CO_2 electrolysis[12]. Furthermore, in the technoeconomic analysis conducted within Sisler et al., the production of ethylene would be US$300 cheaper per tonne of ethylene for the two-step CO_2RR compared with the one-step CO_2RR. For this comparison, they applied the highly optimistic parameters of a very low cell voltage and an FE of over 90%. The analysis shows that, under these conditions, both cases lead to a competitive pricing of ethylene compared with the current ethylene market price[20].

Although there are valid reasons to consider substituting the CO_2RR-to-C_{2+} reaction scheme with CORR-to-C_{2+} in various practical applications, the unique catalyst/electrolyte interfacial conditions, particularly under practical current densities where the local pH starts to deviate a lot from the bulk electrolyte pH, make it challenging to interchange these two reactions. In this Perspective we have methodically

assembled and presented datasets to provide readers with a clearer understanding of this inability to interchange these reactions. In addition, we have illustrated how alterations in the interfacial environment and local pH can impact the selectivity distribution, supported by previous observations and theoretical insights. By providing this Perspective, we aspire to stimulate discourse and encourage further exploration among researchers in the field of CO_2 and CO electroreduction, particularly concerning the industrially relevant reaction conditions of such devices.

Carbonate/bicarbonate chemistry and its influence on microenvironment

(Bi)carbonate formation and crossover at the catalyst/electrolyte interface during CO_2RR electrolysis has recently been acknowledged as one of the main barriers to industrialization of the CO_2RR. Increased efforts to address this problem and improve the efficiency of carbon utilization have illustrated the substantial microenvironmental differences that exist between the CORR and the CO_2RR, which are largely attributed to the formation of carbonate/bicarbonate anions. Figure 1b,c illustrates the catalyst/electrolyte interface on the Cu catalyst during the electroreduction process and elucidates the distinct microenvironments present during the CO_2RR and CORR. For the aqueous CO_2RR and CORR in neutral or alkaline pH electrolytes, the catalyst/electrolyte interfacial pH is elevated due to the hydroxide ions (OH^-) produced, especially under high current densities. The key difference between the CO_2RR and the CORR arises from the thermodynamically favourable reaction between CO_2 and OH^-, or the so-called CO_2 buffering effect[21]. Unreacted CO_2 molecules in the cathode gas stream during the CO_2RR are simultaneously absorbed by locally generated OH^- ions to form bicarbonate or carbonate ions, as shown in the schematic in Fig. 1b, which can mitigate the local pH increase dramatically during CO_2RR electrolysis. Evidence from experiments and simulations suggests that, under practical reaction conditions in electrolysers based on an anion-exchange membrane (AEM), carbonate ions are the dominant ionic species that are formed and cross over the interface instead of bicarbonate ions or hydroxide ions[22,23,28].

By contrast, the CORR lacks pH buffering chemistry due to the absence of an acidic gas (for example, CO_2) at the cathode. Figure 1c shows only a high concentration of hydroxide ions, other than liquid product anions such as acetate, formed at the interface during the CORR. This phenomenon suggests a distinct local pH on the surface of the catalyst for the CO_2RR and the CORR, even when their catalytic material and electroreduction conditions are the same.

Many researchers have identified that such formation of carbonate ions can damage the stability of the CO_2 reduction reaction in electrolysers with gas diffusion electrodes. This chemistry leads to precipitation on the microporous carbon component within the gas diffusion layer, damaging and blocking the system[24,25]. Furthermore, the formed carbonate ions act as the main charge carrier instead of hydroxide ions, which noticeably lowers the conductivity across the AEM, resulting in a higher resistance for the AEM-based electrolyser[26]. Moreover, carbonate formation leads to evident crossover of CO_2 gas, which lowers the carbon utilization during the CO_2RR (refs. 27,28). By contrast, the CORR can avoid such problems related to carbonate formation due to its lack of buffering reaction capability. However, this lack of pH buffering increases the effect of another problem for the CORR compared with the CO_2RR. The high interfacial pH environment in the CORR can affect the stability of the CORR electrolyser by hastening the reconstruction of Cu-based catalysts. As such, CO_2RR and CORR electrolysers demonstrate distinct limitations due to this carbonate chemistry.

During the remainder of this Perspective, we lay our focus on how differences in the microenvironment caused by CO_2 buffering can change the CORR and CO_2RR chemical pathways towards C_{2+} products, despite the shared intermediate before C–C coupling (that is, CO*).

Differences in C_{2+} product distributions between the CO_2RR and the CORR

The differences in the microenvironments at the catalyst/electrolyte interface between the CO_2RR and CORR trigger us to investigate further if their product distributions could be impacted. In the past decade, there have been many studies of both the CO_2RR and CORR on Cu and Cu-derived catalysts for high-value C_{2+} products. In many of these investigations, particularly under practical operation current densities, we have noticed an important re-occurring phenomenon: the CO_2RR is more likely to yield high selectivity for ethylene and ethanol[29–35], whereas the CORR typically leads to high selectivity for acetate[15,16,36–40]. The normalized ratio between acetate versus other C_{2+} products, which does not consider any C_1 products or hydrogen, was plotted for different studies[15,16,29–48], as shown in Fig. 2. This normalized ratio facilitates a direct comparison of the C_{2+} product distribution between different studies, focusing on the reaction after the C–C coupling step. Even though this ratio is appropriate for the purposes of our Perspective, researchers must use these ratio data with caution since the values do not contain any information about the absolute activity towards each product. For a more general and industrially relevant comparison of these performances from the different references, representative selectivity data beyond a current density threshold (>100 mA cm^{-2}) were distinguished from the other data points in Fig. 2a,b. The data and references represented in Fig. 2a,b were selected without considering different electrolytes and setup of gas diffusion electrode electrolyser. The data points were chosen to include the lowest and the highest ratio point within each study. The figure uses two different parameters to calculate the ratio of acetate versus the other C_{2+} products: the FE (Fig. 2a) and the number of moles of products generated (Fig. 2b). Even though these electrochemical studies use various electrolytes ($KHCO_3$, KOH and KCl) and device setups (MEA, flow cell, porous solid electrolyte electrolyser) and have an assortment of copper catalysts, a clear trend is present in the product distributions of these CO_2RR and CORR studies. For both the FE-based acetate ratio and the molar-based acetate ratio, the CO_2RR (Fig. 2a,b, red) is largely aggregated in the low ratio region (<0.1), suggesting that minimal acetate product is produced during electrolysis. The CORR (Fig. 2a,b, blue) is more dispersed, but comparatively shows a much higher ratio of acetate versus other C_{2+} products. In addition, the higher current density regions in the CORR show a higher ratio of the acetate product. Calculating the ratio from the FE or moles of products produced had no impact on the aforementioned trend. From this trend, we hypothesize that the CO_2/carbonate buffering reaction and the local pH difference can be one of the key reasons behind the distinct product disparities between these two reactions. It is important to note that most of the outliers, the CORR with a zero acetate FE ratio or the CO_2RR with a high acetate ratio, occur in the low current density regime, whereas in the industrially relevant current density regime the trend described above is highly apparent. This hypothesis is supported by our observation that the reaction between CO_2 and hydroxide ions is a facile process that readily reduces the local pH of the catalyst surface[49,28]. Therefore, if there is a large concentration of CO_2 gas present, as in the CO_2RR, the local pH at the surface of the catalyst will be restricted according to (bi)carbonate chemistry, regardless of the electrolyte used (even with highly alkaline solutions). This lower local pH can possibly promote the reaction intermediate that goes to ethylene and ethanol. By contrast, during the CORR, the local pH will be influenced greatly by either the bulk electrolyte or the applied current density in the absence of inhibitive pH buffering effects. As a result, acetate products can be promoted in highly alkaline electrolytes or under high current densities, as observed in different studies[36,37,50].

The resulting pattern suggests that the discrepancy in product selectivity transcends the catalyst/device design and attests to the influence of the local pH and interfacial microenvironment on the product-formation pathways. This hypothesis can also be supported by the recent investigation at Dalian National Laboratory for Clean

https://doi.org/10.1038/s41929-023-01082-4

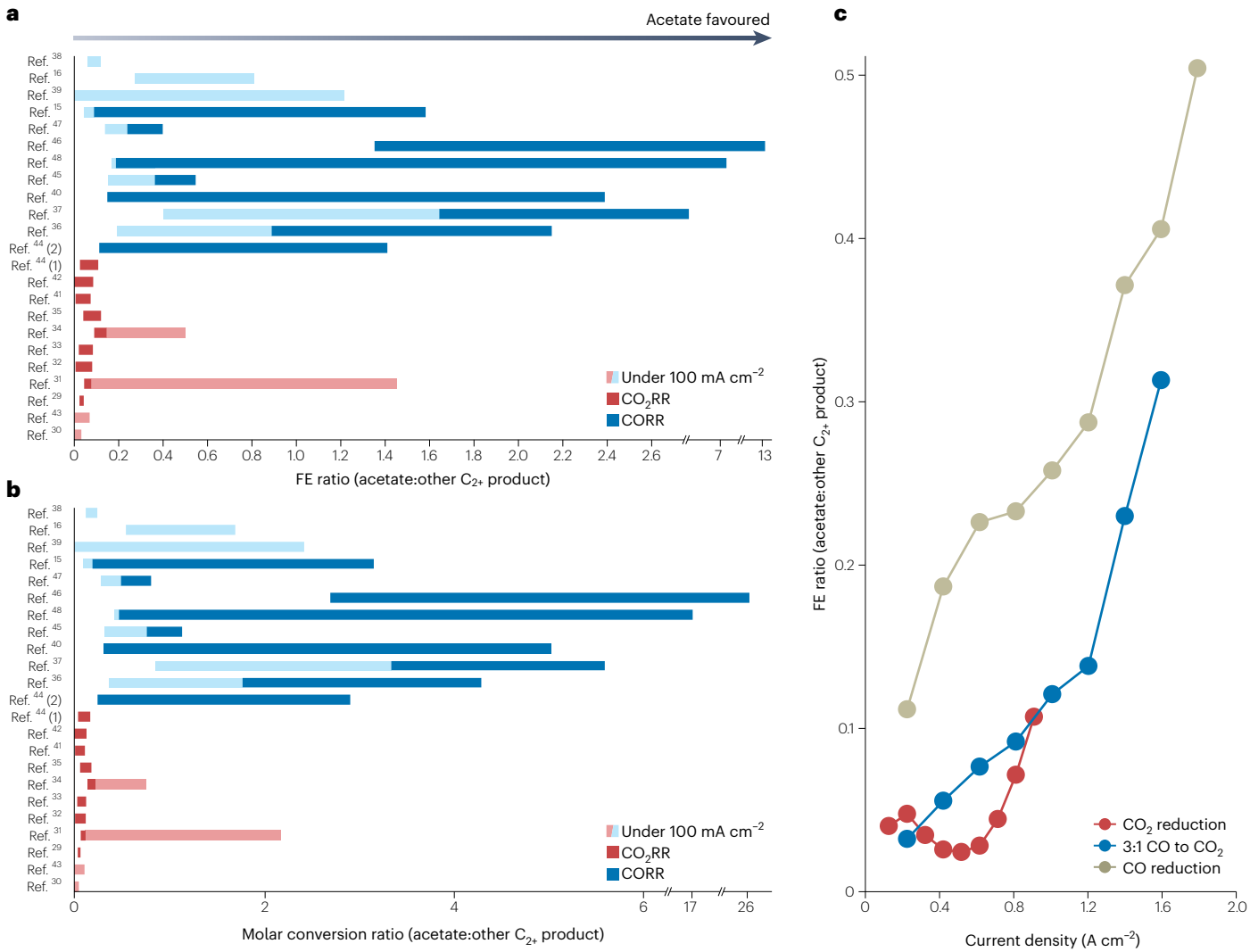

Fig. 2 | Ratio of acetate formation versus other C_{2+} products in the literature. **a**,**b**, Floating bar graph showing the multi-carbon product distributions in the CO_2RR (red) and CORR (blue), where the ratios of acetate versus other C_{2+} product in terms of the FE (**a**) and the number of moles of product (**b**) were calculated for several sample points in each reference. Data points that satisfy the current threshold (>100 mA cm^{-2}) are denoted using a darker colour, and those below the threshold are shown using a lighter colour[15,16,29–48]. **c**, Plot showing the FE ratio of acetate versus other C_{2+} products against the current density for the data of Wei and co-workers[44].

Energy[44]. Figure 2c uses the data of Wei et al. from this laboratory to look at the influence of the input gas composition and the potential on the acetate ratio. Unlike Fig. 2a,b, this demonstration was carried out using the same device and the same catalyst, and shows a more direct comparison between the CO_2RR and the CORR. The data show an increase in the FE acetate ratio as the current density is increased for all three datasets. The higher acetate ratio at higher current density values agrees with our observation since the local pH on the catalyst tends to increase with increasing current density. In the case of the pure CO_2 inlet (red), however, the increase is less visible below 800 mA cm^{-2}. This observation can be associated with the buffering capability of CO_2, which can mitigate the local pH increases resulting from reduction current densities until very high rates. Furthermore, at equal current density values, having CO in the inlet resulted in a higher ratio of acetate versus other C_{2+} products by a noticeable magnitude. The observation from the data of Wei et al. agrees with the local pH phenomenon described above. The excess CO_2 gas present in the CO_2RR or mixed-gas electrolyser can mitigate the local pH increase from electrochemical reduction reactions on the surface. By contrast, the CORR lacks this buffering capability, which results in a higher local pH and acetate ratio. In accordance with our speculation, the cascade CO_2 conversion strategy, which combines the two independent reaction steps of CO_2 to CO and CO to C_{2+}, could behave differently with or without a CO purification step (CO_2 removal) in between[51]. With some remaining CO_2 from the first step co-fed into the downstream CORR reactor, the local pH could still be buffered and the final product distribution could be close to a direct CO_2RR-to-C_{2+} conversion, which may not behave similarly to pure CORR electrolysis. The difference in C_{2+} product selectivity indicates that decoupling the CO_2RR into cascade reactions is incommutable with direct CO_2RR in practice since the preferred product pathway could change.

Some researchers have observed a difference in selectivity between the CO_2RR and the CORR in recent years and associated this observation with reactor kinetics. It is now widely accepted that reactor kinetics heavily influence the C_{2+} product selectivity from Cu-based catalysts. Numerous experts in the field have achieved high C_{2+} FE values by increasing the residence time of CO, specifically surface-adsorbed CO (CO*), through transport adjustments in the electrolyte[52], control of the inlet gas pressure[44] or modulation of the inlet gas composition[44]. Although various chemical mechanisms have been proposed for this effect, it is predominantly believed that increasing the presence of CO* at the Cu catalyst site promotes the C–C coupling process. Recent

research endeavours have made similar claims to illustrate the divergent C_{2+} products arising from the CO_2RR and the CORR[44,53]. Although these studies propose slightly different mechanisms to explain the disparity between CO_2 and CO electrochemical reduction outcomes, a consensus has emerged that attributes the difference to the surface coverage of CO and the reactor design. This reasoning, however, has not been as universally embraced as discussions about its effect on C–C coupling. The precise cause for the variance in C_{2+} product distributions between CO_2 and CO reductions, especially concerning acetate and other C_{2+} products, remains unidentified. In this Perspective, we propose the local environment and pH as potent factors that influence this selectivity between the CO_2RR and the CORR, particularly under high current density regimes. If the CO coverage on active sites predominantly determines acetate formation, we anticipate that the CO_2RR at higher current densities, on an identical copper catalyst, would produce considerable amounts of acetic acid. This is because generally transforming surface-adsorbed CO_2 to surface-adsorbed CO is energetically favourable, with C–C coupling being recognized as rate-limiting[33]. At high current densities, the transformation of surface-adsorbed CO_2 into surface-adsorbed CO would increase the CO coverage since the subsequent C–C coupling step limits the overall reaction rate. Under the above consideration, we would expect a similar active-site environment in both the CO_2RR and CORR cases. However, this is quite different from what has been observed. It could be that the reactor kinetics, catalytic active sites, catalyst morphology, electrolyte pH or electrolyte composition play a substantial role when the applied current density is low. Therefore, the studies and regimes that do not fall into our high current density threshold may have a stronger relationship with the reactor kinetics or many other factors closely tied to catalytic materials, rather than the local pH. However, at high current densities, we expect the local pH to play a more important role in determining the selectivity between the CO_2RR and the CORR. This is further supported by the fact that CORR studies typically reveal an upsurge in acetate selectivity with increasing current density, contradicting the *CO coverage theory that would anticipate a decrease in *CO at the surface with increasing current density (CO consumption rate).

Chemical pathways to acetate and their relationship with local pH

The inherent differences in the microenvironments of the CO_2RR versus the CORR can give rise to distinguishable product selectivity. However, despite evident progress, several aspects of the underlying reduction mechanisms remain uncertain. For the CO_2RR and CORR operated at high current density, proton consumption and hydroxide generation at the surface can yield a pH that greatly exceeds that of the bulk electrolyte. This gradient is a function of several factors, including the bulk pH, the diffusion length to the surface, the presence of buffers (if any) and the rate of reduction reactions, all of which serve to define the differential equations and boundary conditions of transport and reaction kinetics (Fig. 3a). In recent years, the optimization of this gradient has garnered increasing attention because of its implications for the CO_2RR and CORR device performance, for example, the selectivity between C_1 and C_2 products or the suppression of the HER. In general, the CO_2RR and CORR reaction network contains several proposed pathways that can be influenced by proton (or hydroxide) availability. Sensitivity to pH can occur (but does not necessarily occur) if a reaction step involves either proton-coupled electron transfer (PCET) steps or potential-independent chemical steps[54,55].

Here, we highlight the selectivity-determining step(s) (SDS(s)) and pathways of several acetate formation mechanisms from the literature that underscore the importance of local pH. These mechanisms were chosen to represent prevalent bifurcation types in the reduction to acetate (Fig. 3b). Note that these mechanisms are not exhaustive and that the exact reduction pathway(s) remain under debate; we refer the reader to the original articles for a more detailed discussion of each pathway[10,37,56]. Nonetheless, the bifurcation points in the reaction pathways that govern acetate selectivity typically fall under three types: Case 1 is the competition between two PCET steps; Case 2 is the competition between a PCET step and a chemical step; and Case 3 is the competition between two chemical steps. The ability of Cases 1–3 to explain the observable selectivity differences in C_{2+} products remains under debate and has been highlighted in other studies; however, it is worth noting that the pH can have implications in all cases[55–57]. For the CORR, the relevance of these competing possibilities is dependent on a multitude of factors, including those related to the reactor and reaction kinetics. For the CO_2RR at higher current densities, however, selectivity is restricted to non-acetate products and appears irrespective of the reactor or catalyst design (see Fig. 3). Thus, the competition between pathways is tied heavily to the proton (or hydroxide) availability near the surface. In this case, knowledge of the local pH becomes increasingly important to distinguish product selectivity.

For any proposed mechanism involving C_{2+} products, the local pH can play a notable role in the underlying PCET chemistry. Several mechanisms present in the literature involve PCET step(s) at an SDS between acetate and other C_{2+} products, such as those represented in Case 1 and Case 2 (Fig. 3b)[10,36,37,56,58]. For Case 1, there exists a competition between two PCET steps that may have different sensitivities to changes in pH, whereas Case 2 entails a competition between a PCET step and a chemical step that may or may not be dependent on the pH. Note that not all PCET steps are affected similarly by the pH, which depends on the proton donor and other aspects such as equilibrium conditions and kinetic barriers[59]. Nevertheless, the demand for PCET steps can determine the ability to form more reduced species and must be met by a supply of protons. This idea is particularly relevant in the case of C_{2+} product selectivity for the CORR and the CO_2RR where the typical PCET requirements to form ethanol and ethylene are at least twice that of acetate (Fig. 3a). However, the governing mechanism(s) are less clear given the differences in potential proton donors. Water, the most common solvent for the CORR and CO_2RR, is often presumed to be the major proton donor in alkaline/high-current conditions, but it can be outperformed by (or be in competition with) other species in the acidic-to-neutral range[60]. Unlike other proton donors, however, the concentration of water is independent of pH and thus its activity for PCET may only be limited by its dissociation and availability at the surface. Thus, in the formation of more reduced products, whereas the proton availability (that is, the local pH) is almost certainly a limiting factor for most proton sources, when the major proton donor is water the effect of pH is more related to the Butler–Volmer kinetics that govern electrochemical reactions.

In addition to the role of local pH as a driver of proton availability, C_{2+} selectivity may be tuned by the availability of hydroxide in the local environment. The balance of OH^- is determined by the pH gradient, which is governed by aspects related to transport and reaction kinetics as illustrated in Fig. 3a. For the CO_2RR, the consumption of OH^- from (bi)carbonate formation naturally mitigates the development of a hydroxide-rich (and thus a proton-deficient) environment, which can yield more reduced products when water is not the proton donor (that is, under more acidic conditions). Alternatively, if a hydroxide species is a reactant to form acetate, such as in the mechanism proposed by Heenen et al. (Fig. 3b), then the presence of a buffer directly shifts the selectivity away from acetate, which could also explain the general selectivity trend of the CO_2RR and CORR under high current density. In this case, hydroxide availability may be the competing theory that governs the selectivity. Therefore, care should be taken when optimizing C_{2+} selectivity by considering both proton availability and hydroxide availability as separate but valuable entities. So far, the vast majority of fundamental research on the CORR and CO_2RR has focused on conditions that are far removed from commercial relevance, resulting in noticeable kinetic differences when compared with high-performance systems. As a critical next step to maintain a

https://doi.org/10.1038/s41929-023-01082-4

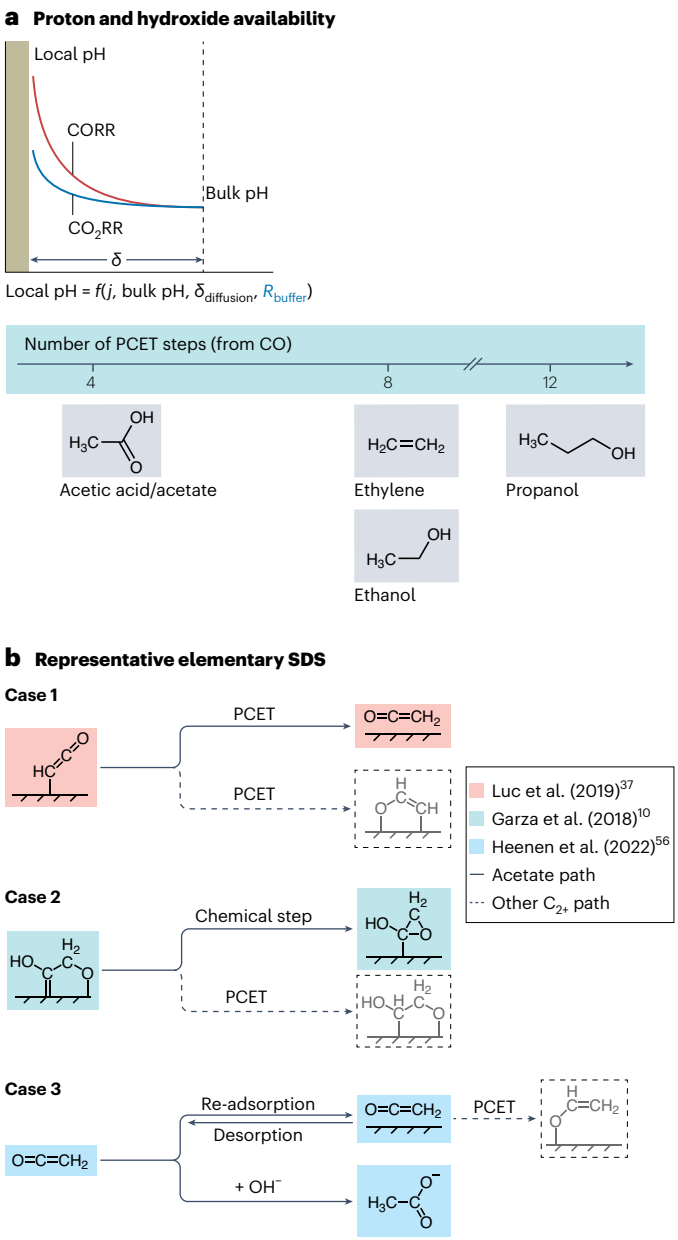

Fig. 3 | Proton/hydroxide availability and bifurcations for acetate formation. **a**, Local pH as a function of the current density (j), bulk pH, diffusion length ($\delta_{diffusion}$) and the resistance of any buffers (R_{buffer}), such as in the CO_2RR; these factors determine the availability of protons for PCET steps to yield acetate, ethanol, ethylene and so on. **b**, Compilation of representative bifurcation points towards acetate and other C_{2+} products. Several proposed mechanisms have key branching points where acetate formation can be influenced by the pH.

balance between theoretical and experimental efforts, it is imperative to develop multi-physics, multiscale models that can begin to account for the nuanced phenomena of the CORR and CO_2RR and describe the selectivity behaviour under high current density. By doing so, we may gain tremendous insight into the driving forces of product selectivity and effectively capture the kinetic costs that develop at scale. Importantly, achieving this goal may require a re-evaluation of existing mechanisms, although it would represent a tremendous leap forward in our understanding of these fundamental processes. Previous studies have concentrated considerable efforts to account for the local pH in the context of the CORR and CO_2RR by combining transport models and density functional theory (DFT) (for example, Fig. 3b, for the mechanism of Heenan et al.), which can yield insights otherwise unknown had a multiscale model not been used[60]. However, (bi)carbonate formation and high current density conditions are seldom modelled in the context of the CO_2RR and even less so in the formation of multi-carbon products. Whereas DFT alone can be used to obtain energies related to many catalytic processes, in lieu of the complex interfacial chemistry and transport limitations that govern high current density CORR and CO_2RR, relying on electronic-scale simulations without considering other physical processes could result in many possible mechanisms—none of which are guaranteed to be correct. Of course, there are aspects other than proton (or hydroxide) availability to be considered when discerning selectivity, such as surface stability and kinetic barriers to the formation of intermediates or undergoing C–C coupling for C_{2+} products such as *n*-propanol. However, proton (or hydroxide) availability can have large implications for some of these processes, and it should not be discounted when using simulation techniques to make approximations, particularly as the field aims for the use of commercially relevant current densities.

Recent CO_2RR technologies and their relationship with the local pH effect

The behaviour of recently developed CO_2RR technologies may be reconciled by a strong relationship with the local pH effect. For example, the pseudo-tandem reaction system reported by Wu and collaborators demonstrated CO_2-to-CO and subsequent CO-to-C_{2+} reactions with a sequence of Ag and Cu catalysts on a single electrolyser in a segmented tandem manner[61]. It showed impressive selectivity for C_{2+} products, especially ethylene. Interestingly, despite the dominant CORR-to-C_{2+} reaction that occurred on the Cu end of the catalyst, acetate was only a minor product. This result contrasts with other Cu-based tandem studies conducted on cascading CO_2RR-to-CO and CORR-to-C_{2+} devices, which suggest that acetate should result from the CORR-to-C_{2+} reaction[12–14]. Nevertheless, the acetate selectivity in these studies was low, which highlights that even though the process is the CORR, the presence of CO_2 in the feed altered the microenvironment and thereby influenced the product selectivity. As shown in Fig. 4a, this observation emphasizes the importance of distinguishing cascade reaction systems that contain product purification steps with the tandem system that carries the remaining CO_2 into the second device. Depending on the target product(s), one must prevent or promote the presence of CO_2 gas during the CORR process to actively control the product distribution while operating these reactor systems.

Moreover, as depicted in Fig. 4b, increasing the single-pass CO_2 utilization efficiency has been of large interest in the field of the CO_2RR (ref. 62). A prevalent idea for improving this efficiency entails limiting the carbonate crossover to the anode and increasing the selectivity of the CO_2RR target product(s). During this process, it is inevitable to decrease the flow rate or concentration of the inlet CO_2 gas to decrease the excess CO_2 in these systems. The amount of CO_2 present in these investigations will determine the extent of (bi)carbonate formation, or the CO_2 buffering capability, and thus the product selectivity. The schematic in Fig. 4b illustrates how the local concentration of CO_2 is largely decreased as it interacts with the catalyst surface. For investigations with decreased flow rates of inlet CO_2, the local pH (and thus the selectivity distribution) of the CO_2RR device must be monitored carefully for conditions that facilitate acetate formation. The same concept can be applied when the feed is sourced from low-concentration CO_2 resources such as flue gas. Similar to the case of a decreased CO_2 flow rate, low CO_2 concentrations will experience a relatively high local pH from the lower CO_2 buffering capacity.

Although this Perspective considers the CO_2 buffering effect in the context of CO_2RR and CORR to distinguish the two reactions, the CO_2 buffering effect has implications for other electrochemical technologies such as oxygen reduction reaction, HER or nitrogen reduction reaction devices (Fig. 4c). At the research level, electrocatalysis studies typically use high-purity reactant gases or liquids as inputs

https://doi.org/10.1038/s41929-023-01082-4

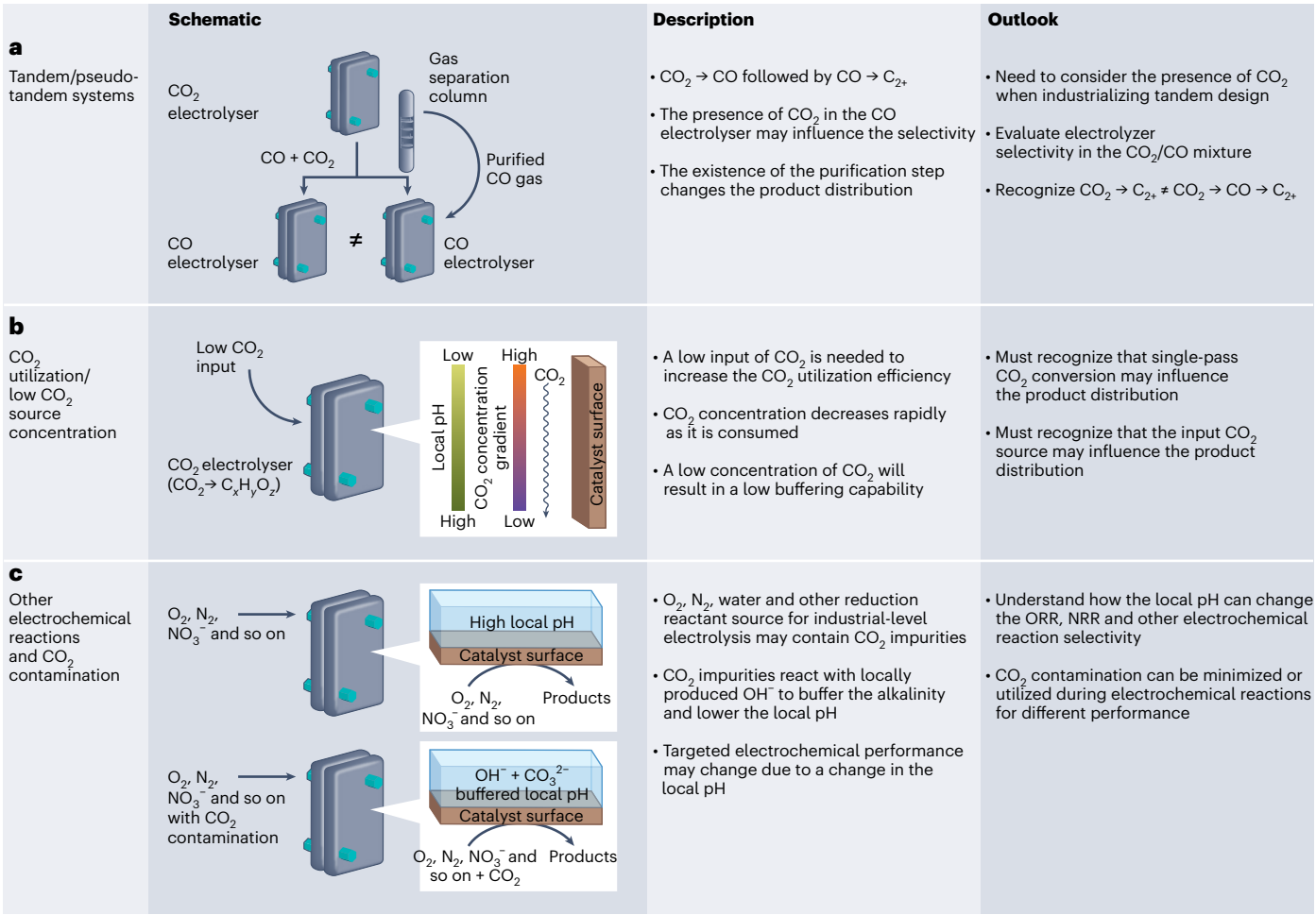

Fig. 4 | Example reactions and reactor designs that can be influenced by the local pH. a–**c**, A graphical schematic, a concise description and an outlook on technologies associated with the selectivity distribution in the CO_2RR/CORR are shown, where the importance of considering local pH and microenvironment-driven selectivity differences is underscored in three key contexts: the design and utilization of CO_2/CO/C_{2+} tandem/pseudo-tandem systems, with or without CO purification (**a**), high CO_2 utilization systems or systems using low CO_2 flow sources (**b**) and various electrolytic reaction systems that may encounter potential CO_2 contamination (**c**). ORR, oxygen reduction reaction; NRR, nitrogen reduction reaction.

into the system to monitor the performance of the electrolysers and catalysts[2–5]. However, the inlet gases of industrial-scale applications may involve an unwanted environmentally abundant gas, CO_2. This contamination could influence the local pH at the cathode of the electrolyser by forming (bi)carbonate ions. One representative example involves the operation of H_2 fuel cells with air as the input at the cathode. Even though the much higher operation potentials of the oxygen reduction reaction can avoid competition with the CO_2RR, the local pH buffering process by the CO_2 impurity may dramatically influence the catalytic performance. As highlighted by the three aforementioned technologies that are sensitive to CO_2 buffering, understanding this effect mechanistically and experimentally may have implications for research areas beyond the CO_2RR.

Research directions for understanding the local pH effect on the $CO_{(2)}$RR

So far, the exact roles of local pH and (bi)carbonate in the reduction pathways for the CO_2RR and CORR remain far from conclusive. First, a more fundamental understanding of the relationship between the bulk and local pH must be made before understanding the microenvironment. Currently, there are studies that alter the bulk pH to tune the selectivity during the electrolysis of CO_2 or CO (refs. 21,49,50). However, few studies are available that systematically investigate the wider range of electrolyte pH (including the acidic region)[21,49]. Generally, it is concluded that an acidic environment yields a lower selectivity for C_{2+} products that include ethylene, ethanol and acetic acid. However, to facilitate effective investigations into the wider range of pH, a selectivity analysis of CO_2 or CO reduction must be conducted while neglecting hydrogen generated from the HER. Namely, the C_{2+} product distribution should be considered exclusively, especially as the bulk pH becomes more acidic. Deriving relationships between the bulk and local pH from absolute values of ethylene or acetic acid formed is challenging due to a propensity for hydrogen evolution in acidic environments. Therefore, we suggest using a product ratio as in Fig. 2 to develop a more general understanding of the dynamics surrounding the bulk pH and reduction pathways. These relationships can be used to deduce the influence of the bulk pH on the local pH and the resulting effect on the product selectivity. Second, a method that can systematically control the OH^- concentration near the catalyst surface is necessary for rigorously testing the local pH effect. Rather than relying on the bulk pH as a vector for controlling the local environment, designing experiments that fine-tune the local pH directly can

unveil its influence on the CO_2RR selectivity distribution with more accuracy and precision. One possibility for achieving this control is the use of CO_2 and CO gas mixtures to maintain the CORR as the dominant reaction while adjusting the local pH of the system with gaseous CO_2. Other acidic gases may also merit consideration to avoid complicated reduction analyses while exercising the same control over the pH. It is worthwhile to note that this CO_2 and CO mixture or acidic gas can be used to study the influence of the local pH on the selectivity. However, this idea does not qualify as being the best solution for selectivity manipulation on an industrial level since it does not properly address the energy efficiency issue that arises with the pH. In this Perspective we have primarily discussed the selectivity change due to the local pH that occurs after the C–C coupling step, although energy efficiency and overpotential have been less considered. However, it is important to understand that the pH will affect the cathode potential, since a higher pH will provide a lower cell potential. With this, future researchers should realize that there is a tradeoff between energy requirement and selectivity due to this local pH for CO_2 or CO electroreduction. The influence of the local pH on the cations should also be investigated further to understand fully how the local pH may influence the electrochemical performance. The hydration sphere around the cation and its facilitation of water-proton donation has been proposed as a convincing mechanism for cation effects in CO_2 or CO reduction[63]. As this process is pH dependent, the local pH may have an influence on this effect. Understanding and investigating this local pH environment further may enable researchers to tune the products of the CO_2RR and CORR more meticulously in the future.

Conclusions

In this Perspective we underscore the distinct microenvironments of the CORR and CO_2RR and highlight the possible effect of (bi)carbonate formation on the local pH and reduction pathways. Many researchers have recognized the substantial implications of the local pH for important electrochemical reactions including the CO_2RR. However, there has been minimal emphasis on the direct role of CO_2 gas in determining the microenvironment and local pH. We would like to stress that while both the CO_2RR and CORR may depend on (surface-bound) CO* to initiate the C–C coupling process, the presence of acidic CO_2 in the CO_2RR inhibits the accumulation of local OH^- and distinguishes the reactions from one another, rendering the reactions incommutable in practical applications. Computational methods that combine ab initio approaches such as DFT with transport models appear to be a reasonable step forward for the community to unravel the dynamics of proton (and hydroxide) availability in the formation of C_{2+} products in high-performance systems. Simultaneous development from the mechanistic to the device level will increase the selectivity of target products and thus prepare the field to address challenges with increasing precision and scale.

Data availability

The data that support the find of this study are available from the corresponding author upon reasonable request.

References

1. De Luna, P. et al. What would it take for renewably powered electrosynthesis to displace petrochemical processes? *Science* **364**, eaav3506 (2019).
2. Fan, L., Xia, C., Zhu, P., Lu, Y. & Wang, H. Electrochemical CO_2 reduction to high-concentration pure formic acid solutions in an all-solid-state reactor. *Nat. Commun.* **11**, 3633 (2020).
3. Dinh, C.-T. et al. CO_2 electroreduction to ethylene via hydroxide-mediated copper catalysis at an abrupt interface. *Science* **360**, 783–787 (2018).
4. Li, J. et al. Copper adparticle enabled selective electrosynthesis of n-propanol. *Nat. Commun.* **9**, 4614 (2018).
5. Pang, Y. et al. Efficient electrocatalytic conversion of carbon monoxide to propanol using fragmented copper. *Nat. Catal.* **2**, 251–258 (2019).
6. Li, C. W. & Kanan, M. W. CO_2 reduction at low overpotential on Cu electrodes resulting from the reduction of thick Cu_2O films. *J. Am. Chem. Soc.* **134**, 7231–7234 (2012).
7. Li, Y. C. et al. Binding site diversity rromotes CO_2 electroreduction to ethanol. *J. Am. Chem. Soc.* **141**, 8584–8591 (2019).
8. Xu, H. et al. Highly selective electrocatalytic CO_2 reduction to ethanol by metallic clusters dynamically formed from atomically dispersed copper. *Nat. Energy* **5**, 623–632 (2020).
9. Ahmad, T. et al. Electrochemical CO_2 reduction to C_{2+} products using Cu-based electrocatalysts: a review. *Nano Res. Energy* **1**, e9120021 (2022).
10. Garza, A. J., Bell, A. T. & Head-Gordon, M. Mechanism of CO_2 reduction at copper surfaces: pathways to C_2 products. *ACS Catal.* **8**, 1490–1499 (2018).
11. Xiao, H., Cheng, T. & Goddard, W. A. Atomistic mechanisms underlying selectivities in C_1 and C_2 products from electrochemical reduction of CO on Cu(111). *J. Am. Chem. Soc.* **139**, 130–136 (2017).
12. Ozden, A. et al. Cascade CO_2 electroreduction enables efficient carbonate-free production of ethylene. *Joule* **5**, 706–719 (2021).
13. Overa, S., Feric, T. G., Park, A.-H. A. & Jiao, F. Tandem and hybrid processes for carbon dioxide utilization. *Joule* **5**, 8–13 (2021).
14. Romero Cuellar, N. S. et al. Two-step electrochemical reduction of CO_2 towards multi-carbon products at high current densities. *J. CO2 Util.* **36**, 263–275 (2020).
15. Jouny, M., Luc, W. & Jiao, F. High-rate electroreduction of carbon monoxide to multi-carbon products. *Nat. Catal.* **1**, 748–755 (2018).
16. Wang, L. et al. Electrochemically converting carbon monoxide to liquid fuels by directing selectivity with electrode surface area. *Nat. Catal.* **2**, 702–708 (2019).
17. Larrazábal, G. O. et al. Analysis of mass flows and membrane cross-over in CO_2 reduction at high current densities in an MEA-type electrolyzer. *ACS Appl. Mater. Interfaces* **11**, 41281–41288 (2019).
18. Song, Y., Zhang, X., Xie, K., Wang, G. & Bao, X. High-temperature CO_2 electrolysis in solid oxide electrolysis cells: developments, challenges, and prospects. *Adv. Mater.* **31**, 1902033 (2019).
19. Zhang, L., Hu, S., Zhu, X. & Yang, W. Electrochemical reduction of CO_2 in solid oxide electrolysis cells. *J. Energy Chem.* **26**, 593–601 (2017).
20. Sisler, J. et al. Ethylene electrosynthesis: a comparative techno-economic analysis of alkaline vs membrane electrode assembly vs CO_2–CO–C_2H_4 tandems. *ACS Energy Lett.* **6**, 997–1002 (2021).
21. Lu, X. et al. In situ observation of the pH gradient near the gas diffusion electrode of CO_2 reduction in alkaline electrolyte. *J. Am. Chem. Soc.* **142**, 15438–15444 (2020).
22. Lin, M., Han, L., Singh, M. R. & Xiang, C. An experimental- and simulation-based evaluation of the CO_2 utilization efficiency of aqueous-based electrochemical CO_2 reduction reactors with ion-selective membranes. *ACS Appl. Energy Mater.* **2**, 5843–5850 (2019).
23. Ma, M., Kim, S., Chorkendorff, I. & Seger, B. Role of ion-selective membranes in the carbon balance for CO_2 electroreduction via gas diffusion electrode reactor designs. *Chem. Sci.* **11**, 8854–8861 (2020).
24. Garg, S. et al. How alkali cations affect salt precipitation and CO_2 electrolysis performance in membrane electrode assembly electrolyzers. *Energy Environ. Sci.* **16**, 1631–1643 (2023).

25. Moss, A. B. et al. In operando investigations of oscillatory water and carbonate effects in MEA-based CO_2 electrolysis devices. *Joule* **7**, 350–365 (2023).
26. Lees, E. W., Mowbray, B. A. W., Parlane, F. G. L. & Berlinguette, C. P. Gas diffusion electrodes and membranes for CO_2 reduction electrolysers. *Nat. Rev. Mater.* **7**, 55–64 (2022).
27. Rabinowitz, J. A. & Kanan, M. W. The future of low-temperature carbon dioxide electrolysis depends on solving one basic problem. *Nat. Commun.* **11**, 5231 (2020).
28. Kim, J. Y. 'Timothy' et al. Recovering carbon losses in CO_2 electrolysis using a solid electrolyte reactor. *Nat. Catal.* **5**, 288–299 (2022).
29. Wang, X. et al. Efficient electrically powered CO_2-to-ethanol via suppression of deoxygenation. *Nat. Energy* **5**, 478–486 (2020).
30. Li, F. et al. Cooperative CO_2-to-ethanol conversion via enriched intermediates at molecule–metal catalyst interfaces. *Nat. Catal.* **3**, 75–82 (2020).
31. García de Arquer, F. P. et al. CO_2 electrolysis to multicarbon products at activities greater than 1 A cm^{-2}. *Science* **367**, 661–666 (2020).
32. Chen, X. et al. Electrochemical CO_2-to-ethylene conversion on polyamine-incorporated Cu electrodes. *Nat. Catal.* **4**, 20–27 (2021).
33. Ma, W. et al. Electrocatalytic reduction of CO_2 to ethylene and ethanol through hydrogen-assisted C–C coupling over fluorine-modified copper. *Nat. Catal.* **3**, 478–487 (2020).
34. Wang, Y. et al. Catalyst synthesis under CO_2 electroreduction favours faceting and promotes renewable fuels electrosynthesis. *Nat. Catal.* **3**, 98–106 (2020).
35. Zhang, X. et al. Selective and high current CO_2 electro-reduction to multicarbon products in near-neutral KCl electrolytes. *J. Am. Chem. Soc.* **143**, 3245–3255 (2021).
36. Zhu, P. et al. Direct and continuous generation of pure acetic acid solutions via electrocatalytic carbon monoxide reduction. *Proc. Natl Acad. Sci. USA* **118**, e2010868118 (2021).
37. Luc, W. et al. Two-dimensional copper nanosheets for electrochemical reduction of carbon monoxide to acetate. *Nat. Catal.* **2**, 423–430 (2019).
38. Chen, R. et al. Highly selective production of ethylene by the electroreduction of carbon monoxide. *Angew. Chem. Int. Ed.* **59**, 154–160 (2020).
39. Li, C. W., Ciston, J. & Kanan, M. W. Electroreduction of carbon monoxide to liquid fuel on oxide-derived nanocrystalline copper. *Nature* **508**, 504–507 (2014).
40. Ji, Y. et al. Selective CO-to-acetate electroproduction via intermediate adsorption tuning on ordered Cu–Pd sites. *Nat. Catal.* **5**, 251–258 (2022).
41. Zhang, J. et al. Accelerating electrochemical CO_2 reduction to multi-carbon products via asymmetric intermediate binding at confined nanointerfaces. *Nat. Commun.* **14**, 1298 (2023).
42. Wu, Z.-Z. et al. Identification of Cu(100)/Cu(111) interfaces as superior active sites for CO dimerization during CO_2 electroreduction. *J. Am. Chem. Soc.* **144**, 259–269 (2022).
43. Wei, X. et al. Highly selective reduction of CO_2 to C_{2+} hydrocarbons at copper/polyaniline interfaces. *ACS Catal.* **10**, 4103–4111 (2020).
44. Wei, P. et al. Coverage-driven selectivity switch from ethylene to acetate in high-rate CO_2/CO electrolysis. *Nat. Nanotechnol.* **18**, 299–306 (2023).
45. Rong, W. et al. Size-dependent activity and selectivity of atomic-level copper nanoclusters during CO/CO_2 electroreduction. *Angew. Chem. Int. Ed.* **60**, 466–472 (2021).
46. Jin, J. et al. Constrained C_2 adsorbate orientation enables CO-to-acetate electroreduction. *Nature* **617**, 724–729 (2023).
47. Ji, Y., Yang, C., Qian, L., Zhang, L. & Zheng, G. Promoting electrocatalytic carbon monoxide reduction to ethylene on copper–polypyrrole interface. *J. Colloid Interface Sci.* **600**, 847–853 (2021).
48. Guo, S. et al. Promoting electrolysis of carbon monoxide toward acetate and 1-propanol in flow electrolyzer. *ACS Energy Lett.* **8**, 935–942 (2023).
49. Ma, M. et al. Local reaction environment for selective electroreduction of carbon monoxide. *Energy Environ. Sci.* **15**, 2470–2478 (2022).
50. Henckel, D. A. et al. Potential dependence of the local pH in a CO_2 reduction electrolyzer. *ACS Catal.* **11**, 255–263 (2021).
51. Gurudayal et al. Sequential cascade electrocatalytic conversion of carbon dioxide to C–C coupled products. *ACS Appl. Energy Mater.* **2**, 4551–4559 (2019).
52. Watkins, N. B. et al. Hydrodynamics change Tafel slopes in electrochemical CO_2 reduction on copper. *ACS Energy Lett.* **8**, 2185–2192 (2023).
53. Ma, W. et al. Electrocatalytic reduction of CO_2 and CO to multi-carbon compounds over Cu-based catalysts. *Chem. Soc. Rev.* **50**, 12897–12914 (2021).
54. Jackson, M. N., Jung, O., Lamotte, H. C. & Surendranath, Y. Donor-dependent promotion of interfacial proton-coupled electron transfer in aqueous electrocatalysis. *ACS Catal.* **9**, 3737–3743 (2019).
55. Kastlunger, G. et al. Using pH dependence to understand mechanisms in electrochemical CO reduction. *ACS Catal.* **12**, 4344–4357 (2022).
56. Heenen, H. et al. The mechanism for acetate formation in electrochemical $CO_{(2)}$ reduction on Cu: selectivity with potential, pH, and nanostructuring. *Energy Environ. Sci.* **15**, 3978–3990 (2022).
57. Wang, L. et al. Electrochemical carbon monoxide reduction on polycrystalline copper: effects of potential, pressure, and pH on selectivity toward multicarbon and oxygenated products. *ACS Catal.* **8**, 7445–7454 (2018).
58. Kuhl, K. P., Cave, E. R., Abram, D. N. & Jaramillo, T. F. New insights into the electrochemical reduction of carbon dioxide on metallic copper surfaces. *Energy Environ. Sci.* **5**, 7050–7059 (2012).
59. Warburton, R. E., Soudackov, A. V. & Hammes-Schiffer, S. Theoretical modeling of electrochemical proton-coupled electron transfer. *Chem. Rev.* **122**, 10599–10650 (2022).
60. Dattila, F., Seemakurthi, R. R., Zhou, Y. & López, N. Modeling operando electrochemical CO_2 reduction. *Chem. Rev.* **122**, 11085–11130 (2022).
61. Zhang, T. et al. Highly selective and productive reduction of carbon dioxide to multicarbon products via in situ CO management using segmented tandem electrodes. *Nat. Catal.* **5**, 202–211 (2022).
62. Xie, Y. et al. High carbon utilization in CO_2 reduction to multi-carbon products in acidic media. *Nat. Catal.* **5**, 564–570 (2022).
63. Marcandalli, G., Monteiro, M. C. O., Goyal, A. & Koper, M. T. M. Electrolyte effects on CO_2 electrochemical reduction to CO. *Acc. Chem. Res.* **55**, 1900–1911 (2022).

Acknowledgements

We acknowledge the support from the National Science Foundation grant no. 2029442, the Welch Foundation Research grant (C-2051-20230405) and the David and Lucile Packard Foundation (grant no. 2020-71371).

Author contributions

J.Y.T.K., C.S., T.S. and H.W. conceived the idea of the Perspective. J.Y.T.K., C.S. and S.H. gathered the data and conducted the literature review.

J.Y.T.K. and C.S. draughted the manuscript and created all of the figures. T.S. and H.W. supervised the project.

Competing interests
The authors declare no competing interests.

Additional information
Correspondence should be addressed to Thomas P. Senftle or Haotian Wang.

Peer review information *Nature Catalysis* thanks Carlos Morales-Guio and the other, anonymous, reviewer(s) for their contribution to the peer review of this work.